J Math Chem (2013) 51:1864–1880
DOI 10.1007/s10910-013-0188-x

ORIGINAL PAPER

# Efficient stochastic simulation of simultaneous reaction and diffusion in a gas-liquid interface

**J. Carrero-Mantilla · S. Duque-Tobón**

Received: 4 March 2013 / Accepted: 2 May 2013 / Published online: 16 May 2013


**Abstract** A stochastic simulation of simultaneous reaction and diffusion is proposed for the gas-liquid interface formed in the surface of a gas bubble within a liquid. The interface between a carbon dioxide bubble and an aqueous solution of calcium hydroxide was simulated as an application example, taken from the integrated production of calcium carbonate. First Gillespie's stochastic simulation algorithm was applied in separate reaction and diffusion simulations. The results from these simulations were consistent with deterministic solutions based on differential equations. However it was observed that stochastic diffusion simulations are extremely slow. The sampling of diffusion events was accelerated applying a group molecule transfer scheme based on the binomial distribution function. Simulations of the reaction-diffusion in the gas-liquid interface based on the standard Gillespie's stochastic algorithm were also slow. However the application of the binomial distribution function scheme allowed to compute the concentration profiles in the gas-liquid interface in a fraction of the time required with the standard Gillespie's stochastic algorithm.

**Keywords** Stochastic simulation · Gillespie method · Reaction-diffusion · Gas-liquid interface

J. Carrero-Mantilla (✉) · S. Duque-Tobón
Chemical Engineering Department, Colombia's National University at Manizales, Carrera 27 64-60, Manizales 170004, Caldas, Colombia
e-mail: jicarrerom@unal.edu.co

*Present Address*
S. Duque-Tobón
Corporación Tecnova, Medellín, Colombia

## 1 Introduction

Gas-liquid interfaces are of industrial interest in bubble column reactors (Figs. 1, 2). But the simulation of gas to liquid diffusion with simultaneous reaction is challenging due to the combination of spatial-dependent and time-dependent differential equations for diffusion and reaction kinetics. However, the Stochastic Simulation Algorithm (SSA) and its variants are a valid alternative to the use differential equations.

The SSA was first proposed by Gillespie to simulate homogeneous, or well-stirred reactive systems [1–4]. In this algorithm the state of the system is represented with small numbers of molecules, which are recalculated in reaction events occurring at time intervals depending on the state of the system. Stochastic simulations are consistent with chemical reactions because they are the result of random molecule collisions. In the same way diffusion is the result of molecular random drifting governed by concentration gradients. Diffusion simulations based on the SSA depend on this analogy between reaction and diffusion [5]. In such simulations the system is divided in homo-

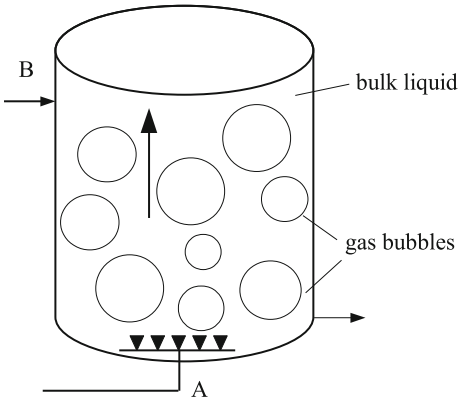


**Fig. 1** Bubble column reactor scheme. Reaction is A + B → C with gas A bubbled in a solution of B

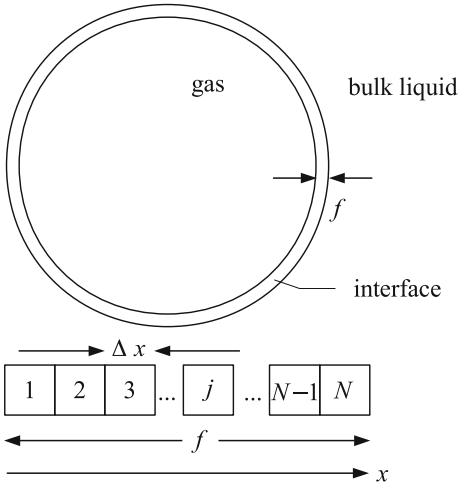


**Fig. 2** Gas-liquid interface in a bubble, divided in *N* subvolumes

geneous sub-volumes, for example this is shown in Fig. 2 for the one-dimensional gas-liquid interface used in this work. Molecule transfers between the subvolumes are included as events analogous to unimolecular reactions [6,7].

Application of SSA to reaction-diffusion systems does not require major modifications, it simply includes two kinds of events, molecule transfer between subvolumes, and reactions within the subvolumes [5,8–11]. In comparison the deterministic approach requires to represent the dependence of concentration on time and distance with differential equations. Although the computation time required to solve that equations is small, its deduction is a non-trivial task that would require more time than the setup of an equivalent stochastic simulation.

Most applications of SSA for diffusion are related to systems of interest in cellular and molecular biology, for example intracellular signaling networks [12], and dendrites [13]. In the field of chemical and process engineering SSA methods are not widespread and have been used mainly to model complex systems such as fluidized beds and processes related with residence time distributions [14]. The lack of stochastic applications to non-biological transport phenomena can be attributed to the nature of the stochastic simulation algorithms. Their execution times are proportional to the number of molecules, and it can make diffusion simulations extremely slow because they use hundreds of molecules distributed in subvolumes. However in systems combining fast diffusion with slow reactions this problem has been addressed transferring groups of molecules in each diffusion event, for example with the Multinomial Simulation Algorithm (MSA) [15]. This suggests that the main non-biological application of stochastic reaction-diffusion can be in small-scale tridimensional systems with complex geometries, difficult to represent with differential equations. But before undertaking simulations of such systems it is necessary to test stochastic methods based on basic laws of diffusion and chemical kinetics in simpler one-dimensional geometries.

In this work we propose the adaptation of the SSA to simulate reaction and diffusion in the gas-liquid interface layer (Fig. 2) between a bubble of carbon dioxide ($CO_2$, A) and an aqueous solution of calcium hydroxide ($Ca(OH)_2$, B). Reaction $A + B \rightarrow C$ produces calcium carbonate ($CaCO_3$, C) which remains in the solution (Fig. 1). This is a well known process, and parameters for both diffusion and reaction are available in Ref. [16]. Moreover, simultaneous diffusion and reaction in this kind of geometry is analyzed in textbooks related with transport phenomena [8,17]. The model for the gas-liquid interface is explained in Sect. 2, the rate of reaction follows a (1,1)-order chemical kinetics, and depends on the diffusion of A through the interface layer.

Separate reaction and diffusion simulations based on the SSA were done before undertaking the simulation of the interface. The results in Sect. 3 coincided with deterministic methods, but it was necessary to improve the speed of the diffusion simulation. To do this the Next Reaction Method (NRM), Ref. [18], and multiple molecule transfers based on the binomial distribution function (BDM), [13,15] were incorporated into the simulations, as described in Sect. 4. Finally, in Sect. 5, the interface was simulated combining SSA with NRM and BDM.

**Table 1** Simulation parameters, from Ref. [16]

| Parameter | Value |
|---|---|
| $\mathcal{D}_A$ | $2.2 \times 10^{-9}\,m^2 \cdot s^{-1}$ |
| $\mathcal{D}_B$ | $1.825 \times 10^{-9}\,m^2 \cdot s^{-1}$ |
| $\mathcal{D}_C$ | $8.517 \times 10^{-10}\,m^2 \cdot s^{-1}$ |
| $f$ | $10^{-5}\,m$ |
| $k$ | $12.4\,m^3 \cdot mol^{-1} \cdot s^{-1}$ |
| $V_e$ | $0.01\,m$ |

## 2 Gas-liquid diffusion model

Calcium carbonate is produced in the reactor shown in Fig. 1. The liquid is an aqueous solution of B and continuous flow of gas A into it generates bubbles. Reaction A+B $\rightarrow$ C and the diffusion of reactants A, B and product C occur in the interface between the bubbles and the bulk liquid. The interfacial film is represented as a flat surface, this is based on the assumption that the bubbles are spherical, with radii much larger than the thickness $f$ of the interfacial film [16,17,19].

Within the interface diffusion occurs in the $x$ direction in Fig. 2. Hence for every species $i$ its concentration ($C_i$) depends on time $t$ and distance $x$ to the gas phase. The form of this dependency is related to the Fick's diffusion law and the rate of reaction in equation

$$\frac{\partial C_i}{\partial t} = \mathcal{D}_i \frac{\partial^2 C_i}{\partial x^2} + \nu_i r \tag{1}$$

where $\mathcal{D}_i$ is the diffusion coefficient for species $i$, and $\nu_i = 1$ for product C and $-1$ for reactants A and B [17,19]. The reaction rate is calculated from the concentration of both reactants in the term $r$ with a (1–1)-order kinetics [20], cited by [16]

$$r = kC_A C_B. \tag{2}$$

Values for reaction and diffusion parameters are shown in Table 1.

Boundary conditions for A, B, and C at the "left" border of the system ($x = 0$ in Fig. 2) are different for every species [16]. The boundary condition for A,

$$C_A = C_{A,0} \tag{3}$$

is of the Dirichlet type because the gas bubble is a source of A and its concentration is considered constant. Neumann boundary conditions are applied for reactant B and product C because their diffusion of into the gas is considered negligible, therefore

$$\begin{aligned} \frac{dC_B}{dx} &= 0, \\ \frac{dC_C}{dx} &= 0. \end{aligned} \tag{4}$$

For the "right" border of the system ($x = f$ in Fig. 2) the boundary condition is related to the variation of the number of moles in the bulk liquid due to reaction and diffusion from the gas. Given that the flux in Fick's law has a direction opposed to the concentration gradient the equation is [16]

$$\frac{\partial C_i}{\partial t} = -\frac{\mathcal{D}_i}{V_e}\left(\frac{\partial C_i}{\partial x}\right) + \nu_i r, \tag{5}$$

where $V_e$ is the specific volume, i.e., the volume of the bulk liquid phase per unit of area of the gas-liquid interface (the units of the flux are $\mathrm{mol/s \cdot m^2}$).

Initial conditions ($t = 0$) are also different for each species. $C_\mathrm{A} = 0$ for $x > 0$ because at $t = 0$ no A molecules have diffused from the gas, but the value at $x = 0$ is $C_{\mathrm{A},0}$. And, given that reaction has not started $C_\mathrm{C} = 0$, and $C_\mathrm{B}$ has the same value as in the bulk liquid.

Both reaction and diffusion equations can be solved separately using analytic and numerical techniques. For reaction the concentrations depend on time according to $r$ defined in Eq. (2),

$$\frac{dC_\mathrm{A}}{dt} = -kC_\mathrm{A}C_\mathrm{B}, \tag{6}$$

with $dC_\mathrm{B}/dt = dC_\mathrm{A}/dt$ and $dC_\mathrm{C}/dt = -(dC_\mathrm{A}/dt)$. The reaction coordinate is calculated from Eq. (6) as

$$\varepsilon = \frac{\exp\left[kt\left(C_{\mathrm{B},0} - C_{\mathrm{A},0}\right)\right] - 1}{\exp\left[kt\left(C_{\mathrm{B},0} - C_{\mathrm{A},0}\right)\right]/C_{\mathrm{A},0} - \left(1/C_{\mathrm{B},0}\right)} \tag{7}$$

and the concentrations are $C_\mathrm{A} = C_{\mathrm{A},0} - \varepsilon$, $C_\mathrm{B} = C_{\mathrm{B},0} - \varepsilon$, and $C_\mathrm{C} = C_{\mathrm{C},0} + \varepsilon$.

The non-stationary diffusion equation in one dimension,

$$\frac{\partial C}{\partial t} = \mathcal{D}\frac{\partial^2 C}{\partial x^2}, \tag{8}$$

can be solved numerically using the Crank-Nicolson (CN) method, a finite difference scheme for partial differential equations [21]. The $\partial C/\partial t$ term is replaced with the forward difference,

$$\frac{C\left(t + \Delta t, x\right) - C\left(t, x\right)}{\Delta t} \tag{9}$$

and $\partial^2 C/\partial x^2$ is the average of central difference approximations,

$$\frac{C\left(t, x + \Delta x\right) - 2C\left(t, x\right) + C\left(t, x - \Delta x\right)}{\left(\Delta x\right)^2}, \tag{10}$$

evaluated at $t$ and $t + \Delta t$ [22,23]. These expressions generate a linear system,

$$\mathbf{U}\mathbf{C}^{t+\Delta t} = \mathbf{V}\mathbf{C}^{t} + \mathbf{W}, \tag{11}$$

which is solved for the concentrations at $t + \Delta t$, i.e. $\mathbf{C}^{t+\Delta t}$. Matrices $\mathbf{U}$ and $\mathbf{V}$ are tridiagonal sparse and its elements are written in terms of the parameter

$$\lambda = \mathcal{D}\frac{\Delta t}{(\Delta x)^2}. \tag{12}$$

In this work the CN method was used to create concentration profiles for diffusion with Dirichlet (constant concentration) and Neumann ($dC/dx = 0$) boundary conditions. In Eq. (11) the constant concentration was represented in the first and last $\mathbf{W}$ elements, while the fictitious boundary method was used for the Neumann condition [23]. Equation 11 was solved using linear algebra routines from the software Scilab.

However the CN method was not applied to the combined reaction-diffusion problem because its formulation is not compatible with the boundary condition for $x = f$. In Eq. (5) the variation $\partial C_i/\partial t$ is the result of the flux crossing the system limit (plus the reaction term), implying that the concentration correspond to a point $N + 1$ outside the interface. It is possible to define the system with such additional point, and to include the reaction term $\nu_i r$ in Eq. (11). But there is a subtle issue, the representation of $\partial^2 C/\partial x^2$ in Eq. (10) assumes that the Fick's diffusion law is valid in the interval from $x - \Delta x$ to $x + \Delta x$. It implies that the whole interval is within the interface. But it is not true if the finite difference equation includes a $N + 1$ point, in this case the interface ends within the interval. It would produce a result inconsistent with the implicit diffusion barrier between interface and bulk liquid.

## 3 Stochastic simulation algorithm

Gillespie's stochastic simulation algorithm (SSA) is based on the definition of possible events within a system. The probability for an event to occur in the next time interval $dt$ is given by the product $a dt$ where the term $a$ is the propensity [4]. The associated probability density function follows an exponential distribution and thus time interval for the next event is calculated as [2]

$$\Delta t = \frac{-\ln(\xi_1)}{\sum_i a_i} \tag{13}$$

from a uniform random number $\xi_1$ and the propensities $a_i$ of the events. For the chemical reaction A+B $\rightarrow$ C an event is the "destruction" of an A, B pair of molecules and the simultaneous "creation" of a C molecule. This is done simply adding one to the number of molecules $M_{\mathrm{C}}$ and subtracting one to $M_{\mathrm{A}}$ and $M_{\mathrm{B}}$. Results from SSA, compared with the deterministic solution (Eq. 7) are shown in Fig. 3.

In this work stochastic simulation algorithm (SSA) was extrapolated to reaction-diffusion systems dividing the space in $N = 100$ subvolumes, see Fig. 2. It was inspired by the use of subvolume arrangements to mimic tissues or cellular structures in the

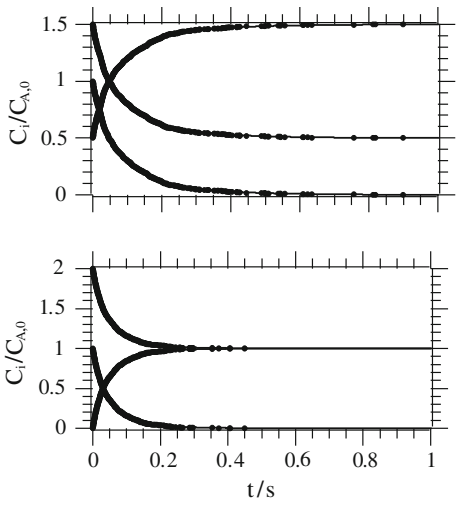


**Fig. 3** Simulation of the reaction A + B → C. *Points*: SSA results with $M_{A,0} = 1000$. *Continuous lines*: analytical formulas. *Upper half* corresponds to the initial conditions $C_{B,0}/C_{A,0} = 1.5$, $C_{C,0}/C_{A,0} = 0.5$, and *lower half* to $C_{B,0}/C_{A,0} = 2$, $C_{C,0}/C_{A,0} = 0$

simulation of biological systems [5,12]. Diffusion was represented with molecule transfers between subvolumes, changing their respective $M$'s. These transfers were allowed only between neighbors, a restriction that has been applied in analogous simulations of intracellular signaling [12]. In fact diffusion stochastic simulations can be devised with molecule transfers between any pair of subvolumes, but it would render the model impractical due to the amount of events needed to sample [15]. The set of subvolumes is analogous to a series of interconnected reactors, or a single reactor with many reaction channels because reaction events occur within them, in addition to the molecule transfers.

The SSA is not a method of solution for differential equations, but both describe the same phenomena. Hence the propensities for reaction ($a_{\mathrm{rx}}$) and diffusion ($a_{\mathrm{dif}}$) are deduced from their associated differential equations. For reaction Eq. (6) is rewritten in terms of $M$'s using the molar concentration definition

$$C_i = M_i / (N_{\mathrm{Av}} V), \tag{14}$$

in this way

$$\frac{dM_{\mathrm{A}}}{dt} = -\frac{k}{N_{\mathrm{Av}} V} M_{\mathrm{A}} M_{\mathrm{B}} \tag{15}$$

where $N_{\mathrm{Av}}$ is the Avogadro's number and the propensity is [2]

$$a_{\mathrm{rx}} = \left(\frac{k}{N_{\mathrm{Av}} V}\right) M_{\mathrm{A}} M_{\mathrm{B}}. \tag{16}$$

In the SSA simulations the volume is fixed, however it is not practical to define its value in advance because an extremely small $V$ is necessary to get reasonable $M_i$ values. Hence the simulation volume was defined indirectly from initial concentrations

(in mol/volume units), and initial numbers of molecules making $N_{\mathrm{Av}} V = (M_i / C_i)_{\mathrm{initial}}$, and replacing its value in Eq. (16).

The diffusion propensity is deduced from the application of Fick's law, flux $= -\mathcal{D}\,(dC/dx)$ [24,25]. The flux is proportional to the number of molecule transfer events occurring per time unit over the area $A$ perpendicular to it. The concentration is $M/(A\Delta x)$, where $\Delta x = f/N$ is the length of the subvolume (see Fig. 2). Replacing the concentration in flux's equation the area cancels out and it gives the propensity [7,12,13,26]

$$a_{\mathrm{dif}} = \frac{\mathcal{D}}{(\Delta x)^2} M. \tag{17}$$

An alternate way to define diffusion propensity is to use $\lambda = \mathcal{D}\Delta t_p / (\Delta x)^2$ where $\Delta t_p$ is an arbitrary time interval (see Eq. 12). In this way

$$a_{\mathrm{dif}} = \frac{\lambda}{\Delta t_p} M \tag{18}$$

and Eq. (13) becomes

$$\frac{\Delta t}{\Delta t_p} = \frac{-\ln(\xi_1)}{2\lambda \sum_i M_i} \tag{19}$$

(the factor 2 appears because the molecule transfers to left or right are separated events, with the same propensity). By using Eq. (19) concentration profiles are associated to $t/\Delta t_p$ values, instead of $t$. Hence results from a single simulation with a given $\lambda$ can be applied to systems with different thickness and diffusivities recalculating $\Delta t_p$ with $\lambda$, $\mathcal{D}$, and $\Delta x$.

Boundary conditions for diffusion are related to the number of molecules or the event propensities. Dirichlet conditions (constant concentration) are applied maintaining $M_i$ constant in the subvolume acting as a molecule source for $i$. In the same way the $C_i = 0$ condition is fulfilled keeping $M_i = 0$. The Neumann condition $dC/dx = 0$ implies no diffusion and hence is represented with a zero propensity.

Reaction and diffusion SSA simulations with 1000 initial molecules were tested comparing their results with values obtained from Eq. (7) (for reaction) and CN method (for diffusion). Reaction simulations (A + B → C) were done with initial conditions $C_{\mathrm{B},0}/C_{\mathrm{A},0} = 1.5$, $C_{\mathrm{C},0}/C_{\mathrm{A},0} = 0.5$, and $C_{\mathrm{B},0}/C_{\mathrm{A},0} = 2$, $C_{\mathrm{C},0}/C_{\mathrm{A},0} = 0$. Diffusion simulations were done for $\lambda = 1$ and $\lambda = 0.2$ and the following initial and boundary conditions: initial zero concentration for $x > 0$, a source in $x = 0$, and Dirichlet or Neumann boundary conditions at $x = f$.

In each case ten simulation runs were done, but in order to not "overcrowd" Figs. 3 and 4 results from all runs were averaged to plot a single series. Additionally for each reaction run results were compared with values calculated with Eq. (7) at each $t$ and the Root Mean Square Deviations (RMSD) was calculated. Figure 3 and maximum and minimum RMSD values in Table 2 show the agreement of SSA with deterministic methods for reaction. For diffusion results in Fig. 4 show the coincidence between

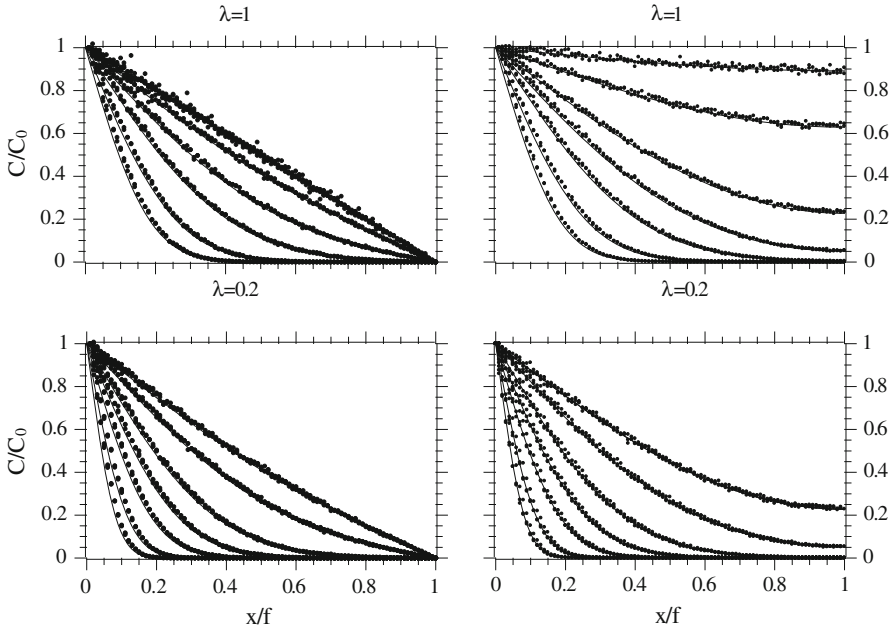


**Fig. 4** Diffusion in one dimension with a source at $x = 0$ for $\lambda = 1$, $\lambda = 0.2$, and $t/\Delta t_p$ =100, 200, 500, 1000, 2000, 5000, and 10 000. *Left plots* correspond to Dirichlet boundary condition, $C\ (t,\ f) = 0$. *Right plots* correspond to the Neumann boundary condition, $dC/dx = 0$ at $x = f$. *Continuous lines* represent the Crank–Nicolson (CN) method results. *Dots* represent results from stochastic simulation algorithm (SSA), next reaction method (NRM), and binomial distribution method (BDM, only for $\lambda = 0.2$)

**Table 2** Minimum and maximum Root Mean Square Deviations (RMSD) from deterministic results for diffusion and reaction stochastic simulations

| Method | Diffusion | | Reaction |
|---|---|---|---|
| | Dirichlet | Neumann | |
| SSA | 0.0169 | 0.0172 | 0.0047 |
| | 0.0262 | 0.0358 | 0.0194 |
| NRM | 0.0174 | 0.0169 | |
| | 0.0266 | 0.0363 | |
| BDM | 0.0150 | 0.0168 | |
| | 0.0337 | 0.0362 | |

stochastic and deterministic CN results. However, a quantitative comparison is difficult due to the dependence of $\Delta t$ on a random number (Eq. 13). It makes the SSA to produce results at time values not uniformly separated, hence they were assigned to the nearest $t/\Delta t_p$ value. Even so the agreement was good, and RMSD values were below 0.05 in all cases (Table 2).

For diffusion in a model with many subvolumes SSA requires execution times that can be several orders of magnitude bigger than in the case of a simple reactive system [12]. This is caused by the huge number of possible events in a diffusion simulation, compared with the reaction case. For example, in our model there are 100 subvolumes, and each one has diffusion (to left or right) and reaction, totaling 300

**Table 3** Averaged execution times and number of events for diffusion simulations with stochastic simulation algorithm (SSA), next reaction method (NRM), and binomial distribution method (BDM)

| Method | Boundary cond. | Time (s) | | Number of events / $10^8$ | |
|---|---|---|---|---|---|
| | | $\lambda = 1$ | $\lambda = 0.2$ | $\lambda = 1$ | $\lambda = 0.2$ |
| SSA | Dirichlet | 1503 | 199 | 9.188 | 1.298 |
| | Neumann | 2574 | 216 | 13.92 | 1.364 |
| NRM | Dirichlet | 2112 | 297 | 9.190 | 1.297 |
| | Neumann | 3184 | 310 | 13.90 | 1.364 |
| BDM | Dirichlet | | 2 | | |
| | Neumann | | 5 | | |

Simulations were run on a Intel Xeon E5410 processor

events. In comparison a reactive system may include 10 independent reactions or less. The number of terms in the sum of propensities, $\sum_i a_i$, is equal to the number of events in the system, hence its value is bigger in the diffusion case, and it produces small $\Delta t$ values from $\Delta t = -\ln(\xi_1) / \sum_i a_i$ (Eq. 13). As a consequence it is necessary to use many more time-steps to cover the same total simulation time.

Results in Table 3 show that the time required to complete diffusion stochastic simulations depends on the parameter $\lambda$ and the boundary conditions (all stochastic simulations were programmed in the same way, FORTRAN 95 code compiled for 64 bit systems). Simulations with smaller $\lambda$ values complete the simulation with less time steps because $\Delta t$ is inversely proportional to $\lambda$ (Eq. 19). It caused that execution times for $\lambda = 1$ were of one order of magnitude bigger than those for $\lambda = 0.2$. With a molecule source at $x = 0$ the Neumann condition produces more molecules in the subvolumes close to $x = f$ than the Dirichlet condition (see Fig. 4). With higher $M_i$ values $\Delta t$ becomes smaller, slowing down the simulation. Hence Neumann simulations were slower than Dirichlet ones, although their execution times were of the same order of magnitude.

## 4 Accelerating stochastic simulations

The Next Reaction Method (NRM) is a scheme to improve the efficiency of the SSA simulations reducing the number of random number generations and its associated computation time. It was proposed by Gibson and Bruck after the First Reaction Method (FRM) that appeared in one of Gillespie's seminal papers [1,18]. In FRM the expected time of occurrence for a single event,

$$t_p = -\ln(\xi)/a + t, \tag{20}$$

is defined as its "putative time". The event with the smallest $t_p$ is selected, and after it propensities and putative times are recalculated with new random numbers. The NRM is essentially an improved FRM that reuses $t_p$ values whenever possible instead of recalculating all them [18]. In every time-step the events whose propensity changes

are identified using a dependence graph, and their putative times are rescaled according to

$$t_p := \left(\frac{a_{\text{old}}}{a_{\text{new}}}\right)(t_p - t) + t. \tag{21}$$

Events with $a = 0$ are assigned an infinite $t_p$ [18, note 11].

The NRM was developed for complex reaction models, for example those describing gene expression [27], and has been applied as a spatial-NRM to multidimensional models for intracellular signaling [12]. The one-dimensional reaction-diffusion model used in this work is much more simpler than the aforementioned examples. The reaction events occur within the subvolumes, and for diffusion events propensities and putative times need only to be recalculated for the two subvolumes involved, therefore the event dependence graph is reduced to the links between the subvolumes and their immediate neighbors.

The results in Fig. 4 and Table 2 show agreement between stochastic NRM simulations and the deterministic CN method. But nevertheless the efficiency of the stochastic simulations was not improved. Their averaged execution time in Table 3 is higher than the value for the SSA simulations in all cases, although there was no significant difference between the number of events required by both methods. It implies that the speed advantage of the next reaction method in complex geometries is lost for one-dimensional simulations. Indexed event queues make NRM faster by avoiding redundant calculations [5], but its effect is lost when the interdependence of events is very simple, as it happens in the one-dimensional system in Fig. 2. Due to the need to recalculate putative times in neighbor subvolumes for every transfer event NRM is handicapped with hundreds of events in the same way SSA is. It suggests that the simulation efficiency can only be improved using a simulation strategy based on the transfer of molecule groups instead of individual molecules. But this approach changes the problem outline, instead of calculating the time between transfers it implies to calculate the number of molecules to be transferred in a predefined time step.

The molecule group transfer strategy was implemented here as a Binomial Distribution Method (BDM) following the procedures proposed by Blackwell [13], and Lampoudi et al. [15]. The transfers were limited to neighbor subvolumes because allowing transfers between non-adjacent subvolumes is not practical. Using a "diffusion radius" of 2 or more would require too many samples of the binomial distribution per time step [15]. The number of molecules to be transferred depends on the binomial probability distribution function,

$$\mathcal{P}(M, n) = \frac{M!}{(M-n)!}(p_m)^n (1 - p_m)^{M-n}. \tag{22}$$

It gives the probability $\mathcal{P}$ of selecting $n$ out of $M$ molecules in the subvolume. $p_m$ is the transfer probability for a single molecule, calculated as the sum of the transfer probabilities to the left (l) or right (r) neighbor subvolumes

$$p_m = p_{\text{l}} + p_{\text{r}}. \tag{23}$$

These probabilities come from the propensities calculated for a single molecule in the form $p = a\Delta t$, where $\Delta t$ is a fixed time interval. For diffusion between internal subvolumes Eqs. (17) and (12) give

$$p = \frac{\mathcal{D}}{(\Delta x)^2}\Delta t, \tag{24}$$

and $p = \lambda$ for simulations defined with such parameter. Where a boundary condition implies a zero propensity the probability is $p = 0$.

The time in a BDM simulation is advanced by adding $\Delta t$, this allows to produce results for exactly the same $t$ values in different runs. In every time-step $n$ is calculated generating a random number to select the $n$ such that $\xi \leq \mathcal{P}(M, n)$. Given $n$ it has been proposed to simply transfer $n/2$ molecules to the left and $n/2$ to the right when $p_\mathrm{l} = p_\mathrm{r}$ [13]. Such choice would be valid, albeit not strictly stochastic. Instead, in this work the numbers of molecules to be transferred to each side $(n_\mathrm{l}, n_\mathrm{r})$ were calculated repeating the procedure described for $n$, but assigning $M \leftarrow n$, $n \leftarrow n_\mathrm{l}$, and $p_m \leftarrow p_\mathrm{l}$ in Eq. (22). Here $p_\mathrm{l}$, $p_\mathrm{r}$ are the transfer probabilities to left and right, and $n_\mathrm{r} = n - n_\mathrm{l}$.

Binomial distribution method simulations for one-dimensional diffusion were set with $\Delta t = 10^{-6}\,\mathrm{s}$ and a fixed molecule transfer probability $p = 0.2$, as in Ref. [13]. With $f = 10^{-5}\,\mathrm{m}$ and $\Delta x = f/100 = 10^{-7}\,\mathrm{m}$ it implies a diffusivity $\mathcal{D} = 2 \times 10^{-9}\,\mathrm{m}^2 \cdot \mathrm{s}^{-1}$. These parameters are consistent with the values in Table 1, and the restrictions [11,15,28]

$$\Delta x \gg (k/\mathcal{D}), \tag{25}$$

and

$$\Delta t \leq \sqrt{\varepsilon}\frac{(\Delta x)^2}{\mathcal{D}} \tag{26}$$

for an error level $\varepsilon = 0.05$, which gives a maximum limit of $1.02 \times 10^{-6}\,\mathrm{s}$. $\mathcal{P}$ values were calculated following the procedure described in Ref. [29], and they were stored in tables corresponding to the $M, n$ pairs to avoid recalculating them [13].

Diffusion results from BDM with Dirichlet and Neumann conditions coincided with those from the deterministic CN method, and SSA and NRM stochastic methods, see Fig. 4 and Table 2. As expected results in Table 3 show that BDM is much more faster than the other stochastic methods. Diffusion simulations done with BDM took in average 0.01 (Dirichlet condition) and 0.02 (Neumann condition) of the SSA time. This is not a very surprising result considering the transfer of several molecules in every step, in opposition to the single transfer of the SSA and NRM.

## 5 Reaction-diffusion simulation

Reaction-diffusion simulations based on SSA include three possible events in each subvolume: reaction, transfer to the left, or transfer to the right. In this work both the

kind of event and the subvolume were selected at each time step generating a single random number $\xi_2$. The propensities were kept in a matrix of the form

$$\begin{bmatrix} a_{11} & a_{12} & & a_{1N} \\ a_{21} & a_{22} & & a_{2N} \\ \vdots & \vdots & \ddots & \\ a_{E1} & a_{E2} & & a_{EN} \end{bmatrix}$$

where $a_{ij}$ is the propensity of the event $i$ in the subvolume $j$, and $E = 3$ is number of possible events in the subvolume. Within a nested double loop the pair $kl$ that fulfills the condition

$$\xi_2 \left( \sum_{i=1}^{E} \sum_{j=1}^{N} a_{ij} \right) \leq \sum_{i=1}^{k} \sum_{j=1}^{l} a_{ij}, \tag{27}$$

gives the event (row $k$) and subvolume (column $l$). The same scheme, without reaction propensities ($E = 2$), was used for diffusion SSA simulations.

Reaction propensities were calculated in the same way described for the diffusion simulations (Eq. 16) using $N_{\mathrm{Av}} V = (M_{\mathrm{A}}/C_{\mathrm{A}})_{x=0}$. The source of A at $x = 0$ implies that $C_{\mathrm{A}}$ ($x = 0$) is constant (Eq. 3), it was applied keeping $M_{\mathrm{A},1}$ unchanged for reaction or molecule transfer events in the first subvolume ($x = 0$, Fig. 2). Similarly bulk fluid was treated as a source of B by keeping constant its number of molecules in the $N$ subvolume. The Neumann conditions in Eq. (4) imply a diffusion barrier between the gas an the interface layer. They were applied assigning a propensity $a = 0$ for B or C molecule transfer events from the first subvolume to the left. The boundary condition for diffusion between interface and bulk liquid depends on the term $(\mathcal{D}_i / V_e)\,(\partial C_i / \partial x)$ in Eq. (5) [8,11]. The propensity for the associated molecule transfer events,

$$a_{\mathrm{dif}} = \frac{\mathcal{D}}{V_e \Delta x} M, \tag{28}$$

was deduced following the same reasoning used for Eq. (17).

Reaction-diffusion simulations of the gas-liquid interface were run for $0 \leq t \leq 0.5$s with the same $N = 100$ subvolumes and the parameters in Table 1. Initial concentrations and numbers of molecules were $C_{\mathrm{A},0} = 1.0\,\mathrm{mol \cdot m^{-3}}$ with $M_{\mathrm{A},0} = 200$ in the first subvolume (as explained before it was kept constant), $C_{\mathrm{B},0} = 5.0\,\mathrm{mol \cdot m^{-3}}$ with $M_{\mathrm{B},0} = 1000$ in every internal subvolume, and $C_{\mathrm{C},0} = 0$. The SSA simulations are extremely slow due to the sampling of all molecule transfers as separate events, they required in average 24 h with a system based on the Intel Xeon E5410 processor, or 18 h with an Intel core-i7 processor. Hence the reaction-diffusion SSA can be considered a method of brute force.

The performance of reaction-diffusion simulations is improved using fixed times for diffusion events, combined with Gillespie's SSA for reactions. This scheme appears in the operator split method by Rodriguez et al. [30], and the multinomial simulation algorithm (MSA) by Lampoudi et al. [15]. The MSA was chosen because it uses the

binomial probability distribution function (Eq. 22) for multiple molecule transfers. The results in Sect. 4 (Table 3 ) show that this BDM-based diffusion increases the efficiency of the simulation. Hence in this work the MSA scheme was adapted combining the binomial distribution method for diffusion with the stochastic simulation algorithm for reaction (BDM-SSA), and with the next reaction method (BDM-NRM).

With simultaneous fast diffusion and slow reactions several diffusion events can occur in the time lapses between reactions. Therefore diffusion events were sampled much more frequently than the reactions using for diffusion a $\Delta t$ smaller than the time between reaction events. Following MSA reaction events were executed separately, but reactants are removed before the diffusion and the products are added after it to prevent the transfer of molecules not yet added, or already removed [15]. For the diffusion (BDM) part of the simulation $\mathcal{P}(M, n)$ tables were used, with $p$ values from Eq. (24) for molecule transfers between internal subvolumes, and

$$p = \frac{\mathcal{D}}{V_e \Delta x} \Delta t \tag{29}$$

between interface and bulk liquid (see Eq. 28). An additional safeguard checked the error level defined in Eq. (26), it was observed in the simulations that $\mathcal{O}(\Delta t) \approx 10^{-8}$ s, corresponding to $\varepsilon \ll 0.001$ (see Eq. 26).

Results from the three simulation methods, SSA, BDM+SSA, and BDM+NRM coincided in Fig. 5. Additionally, the differences between their results were quantified using a mean deviation from the average, defined as

$$\mathrm{MDA}(y) = \sqrt{\frac{1}{N} \sum\nolimits_{i=1}^{N} \left(y_i - \bar{y}_i\right)^2} \tag{30}$$

where $y_i$ is the value $C/C_{\mathrm{A},0}$ for A, B, or C in subvolume $i$, and $\bar{y}_i$ is the average value from the three methods. For each species the MDA was calculated at $t\,(\mathrm{s}) = 0.001$, 0.002, 0.005, 0.01, 0.02, 0.05, 0.1, 0.15, 0.2, 0.30, 0.35, 0.40, 0.45, 0.50 and maximum and minimum values in Table 4 show the agreement between the three simulation methods. In average the BDM-NRM variant took 0.171 of the time required by the SSA, and the BDM-SSA 0.172; that is 3–4 h with the same systems. It shows that the choice of SSA or NRM for the reaction events has little or no effect on simulation speed for reaction-diffusion. The increased efficiency of both BDM-SSA and BDM-NRM is mostly due to the application of BDM. This is consistent with the difference of more than one order of magnitude between the numbers of reaction and diffusion events [15].

During the simulation the combined effects of reaction and diffusion created the concentration profiles shown in Fig. 5. The behavior of the whole interface film was analogous to an hypothetical reactor with an input of gas A at $x = 0$. Diffusion predominated for species A because the continuous feed of its molecules from the gas source at $x = 0$ compensated its deletion in the reaction events. Due to this during the beginning of the simulation the result was similar to the diffusion simulations with the Neumann condition (Fig. 4). As the simulation advanced the feed from the

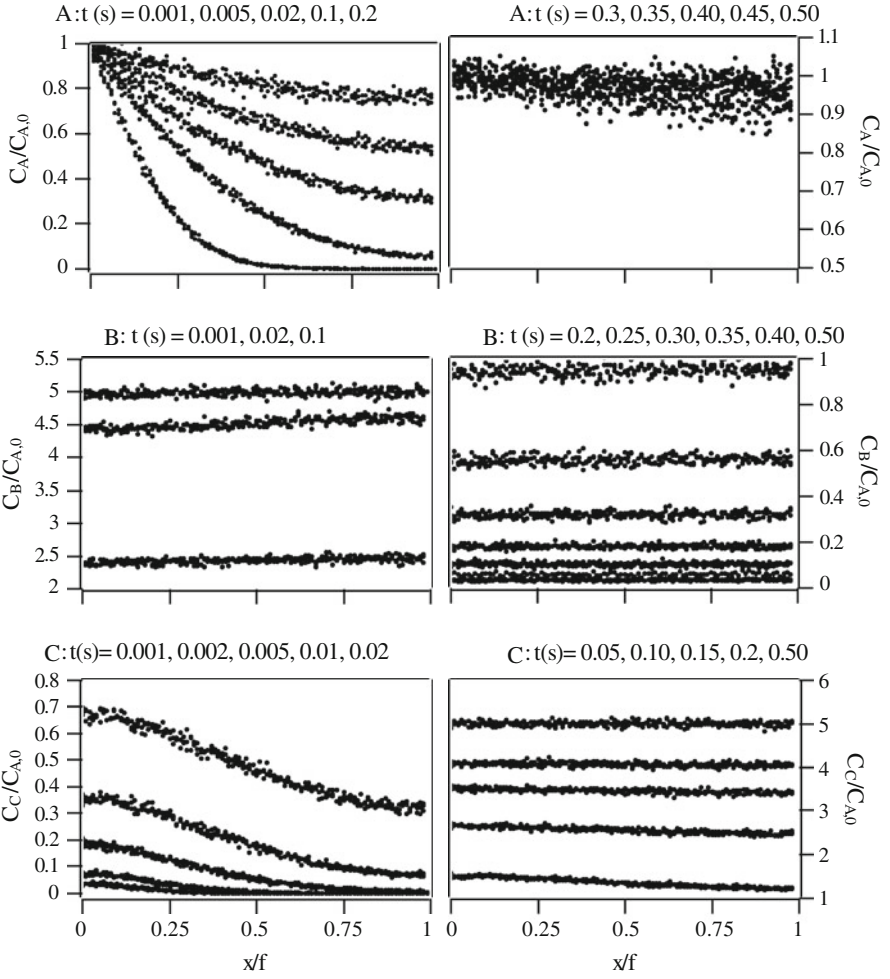


**Fig. 5** Concentration results for reaction-diffusion with stochastic simulation algorithm (SSA), and binomial distribution method (BDM+SSA and BDM+NRM variants). *Each row* includes two plots for the same species at different times. *First row* is for A, second for B, and third for C. The values are divided by the initial concentration of A, $C_{A,0}$

**Table 4** Minimum and maximum mean deviations from the average (Eq. 30) for reaction-diffusion

| Method | Variable ($y$) $C_A/C_{A,0}$ | $C_B/C_{A,0}$ | $C_C/C_{A,0}$ |
|---|---|---|---|
| SSA | 0.0079 | 0.0033 | 0.0015 |
| | 0.0194 | 0.0392 | 0.0446 |
| BDM+SSA | 0.0076 | 0.0035 | 0.0014 |
| | 0.0189 | 0.0453 | 0.0452 |
| BDM+NRM | 0.0068 | 0.0036 | 0.0017 |
| | 0.0201 | 0.0418 | 0.0428 |

gas spreaded A molecules over the entire interface film, and its concentration values tended to $C_{A,0}$.

Species B was consumed in the reaction $A + B \rightarrow C$, but its concentration profiles were not governed by the diffusion of reactant A. Instead, due to the fast diffusion they were almost flat during the entire simulation. In every subvolume the occurrence of reaction events changes the number of B molecules, but it was quickly compensated with transfers from the neighbor subvolumes because many more transfers occur per time unit than reactions.

The number of C molecules in a given subvolume depends on the availability of A and B molecules because it is the product of the reaction. The initial conditions imply that there are B molecules in all subvolumes, but not A ones. As a result during the beginning of the simulation the reaction was governed by the diffusion of A. It acted as limiting reactant close to the source at $x = 0$, hence $C_C$ was higher in the left side of the interface film due to the availability of A molecules.

By the end of the simulation the product C was uniformly dispersed in the film, but its concentration tended to the value $C_{B,0}$. Given that the system has a source of A it indicates that species B acted as a limiting reactant in this part of the simulation. Reaction events proceeded until subvolumes were depleted of B molecules, and the bulk liquid did not act as a source of "fresh" molecules. The cause is that molecule transfers across the interface-liquid boundary are much less probable than within the interface due to the difference between the specific volume $V_e$ and $\Delta x$ (see Table 1). The effect of these parameters can be seen comparing the propensities for a molecule transfer within the interface ($a_{\mathrm{dif},j}$), and between the interface and the bulk liquid ($a_{\mathrm{dif},N}$). Using the same $M$ in Eqs. (17) and (28) it is obtained $a_{\mathrm{dif},j}/a_{\mathrm{dif},N} = V_e/\Delta x = 10^5$, implying that transfers within the interface film can be 100 000 times more likely to occur than transfers across its limit with the liquid. Without diffusion of new molecules from the liquid $C_B$ decreased during the simulation, even near $x = f$ and this limited the production of C.

## 6 Conclusion

It is feasible to simulate simultaneous reaction and diffusion in a gas-liquid interface using stochastic methods in a desktop computer. However application of the standard stochastic simulation algorithm to this problem produces excessively slow simulations. It makes necessary to combine SSA with acceleration techniques, such as the next reaction method or the binomial distribution method, for the diffusion part of the simulation. It was found that the application of NRM has no advantage over SSA for this system because it does not require indexed event queues. But the execution times are vastly reduced by using the BDM for multiple molecule transfers.

The combination of methods proposed in this work improves the efficiency of stochastic simulations but anyway it requires more execution time than the solution of differential equations. For biological systems this handicap has been accepted because they are not amenable to the simulation with deterministic methods. This argument could not be valid with other diffusion-related problems, however, the main reason to apply stochastic methods is not their speed but their adaptability. They can accept

different kinds of events into a single repetition structure, and differential equations and boundary conditions are simply translated into propensities. It means that stochastic simulations require less time to formulate the problem and program its solution, and it can compensate their slow speed. It suggests that stochastic simulations formulated with the BDM or its equivalent are feasible for more complex geometries in reaction-diffusion systems of industrial interest, particularly in cases where the application of differential equations result very difficult.

**Acknowledgments** This work was financed with a Colciencias grant (Programa de Jóvenes Investigadores, convenio 704 Universidad Nacional) for S. Duque-Tobón. The authors wish to thank Matthew Wahl for his assistance and support in the redaction of this article.

## References

1. D.T. Gillespie, J. Comput. Phys. **22**, 403 (1976)
2. D.T. Gillespie, J. Phys. Chem. **81**, 2340 (1977)
3. D.T. Gillespie, J. Stat. Phys. **16**, 311 (1977)
4. D.T. Gillespie, Annu. Rev. Phys. Chem. **58**, 35 (2007)
5. J. Elf, M. Ehrenberg, Syst. Biol. **1**, 230 (2004)
6. F. Baras, M.M. Mansour, Phys. Rev. E **54**, 6139 (1996)
7. D. Bernstein, Phys. Rev. E **71**, 041103 (2005)
8. R. Erban, S.J. Chapman, Phys. Biol. **4**, 16 (2007)
9. P. Lecca, L. Dematte, Intern. J. Biol. Med. Sci. **4**, 211 (2009)
10. A.B. Stundzia, C.J. Lumsden, J. Comput. Phys. **127**, 196 (1996)
11. S.A. Isaacson, C.S. Peskin, SIAM J. Sci. Comput. **28**, 47 (2006)
12. J. Elf, A. Doncic, M. Ehrenberg, in *Fluctuations and noise in biological, biophysical, and biomedical systems*, ed. by S.M. Bezrukov, H. Frauenfelder, F. Moss, SPIE Proc. **5110**, 114 (2003)
13. K.T. Blackwell, J. Neurosci. Methods **157**, 142–153 (2006)
14. H.G. Dehling, T. Gottschalk, H.A.C. Hoffmann, *Stochastic Modelling in Process Technology* (Elsevier, Amsterdam, 2007)
15. S. Lampoudi, D.T. Gillespie, L.R. Petzold, J. Chem. Phys. **130**, 094104 (2009)
16. S. Wachi, A.G. Jones, Chem. Eng. Sci. **46**, 1027 (1991)
17. R.B. Bird, W.E. Stewart, E.N. Lightfoot, *Transport Phenomena* (Wiley, New York, 1960)
18. M.A. Gibson, J. Bruck, J. Phys. Chem. A **104**, 1876 (2000)
19. I. Tosun, *Modelling in Transport Phenomena* (Elsevier, Amsterdam, 2002)
20. V.A. Juvekar, M.M. Sharma, Chem. Eng. Sci. **28**, 825 (1972)
21. J. Crank, P. Nicolson, Math. Proc. Camb. Philos. Soc. **43**, 50 (1947)
22. S.C. Chapra, R.P. Canale, *Numerical Methods for Engineers*, 5th edn. (McGraw-Hill, New York, 2005)
23. M.E. Davis, *Numerical Methods & Modeling for Chemical Engineers* (Wiley, New York, 1984)
24. U.S. Bhalla, Biophys. J. **87**, 733 (2004)
25. U.S. Bhalla, Biophys. J. **87**, 745 (2004)
26. S.A. Isaacson, J. Phys. A: Math. Theor. **41**, 065003 (2008)
27. A. Arkin, J. Ross, H.H. McAdams, Genet. **149**, 1633 (1998)
28. S.A. Isaacson, SIAM J. Appl. Math. **70**, 77 (2009)
29. W.H. Press, B.P. Flannery, S.A. Teukolsky, W.T. Vetterling, *Numerical Recipes in FORTRAN: The Art of Scientific Computing*, 2nd edn. (Cambridge University Press, New York, 1992)
30. J.V. Rodríguez, J.A. Kaandorp, M. Dobrzynski, J.G. Blom, Bioinforma. **22**, 1895 (2006)